Plant Ecology (2023) 224:1059–1073
https://doi.org/10.1007/s11258-023-01361-x

Tree hydrological niche acclimation through ontogeny in a seasonal Amazon forest

Mauro Brum[1] · Luciana F. Alves[2] · Raimundo C. de Oliveira-Junior[3] · Victor Hugo Pereira Moutinho[4] · Natalia Restrepo-Coupe[1] · Karoline Chaves[5] · Deliane Penha[6,7] · Neill Prohaska[1] · Plínio Barbosa de Camargo[8] · Grazielle Sales Teodoro[5] · Sebastião Ribeiro Xavier Júnior[9] · Scott C. Stark[10,11] · José M. S. Moura[6] · Rodrigo Silva[6] · Rafael S. Oliveira[12] · Scott R. Saleska[1]

Received: 6 April 2023 / Accepted: 2 October 2023 / Published online: 5 November 2023

Abstract

How tropical plants cope with water availability has important implications for forest resilience, as severe drought events are expected to increase with climate change. Tree size has emerged as a major axis of drought vulnerability. To understand how Amazon tree species are distributed along size-linked gradients of water and light availability, we tested the niche acclimation hypothesis that there is a developmental gradient in ontogenetic shift in embolism resistance and tree water-use efficiency among tree species that occurs along the understory-overstory gradient. We evaluated ontogenetic differences in the intrinsic water-use efficiency (iWUE) and xylem hydraulic traits of abundant species in a seasonal tropical forest in Brazil. We found that saplings of dominant overstory species start with a high degree of embolism resistance to survive in a dense understory environment where competition for water and light among smaller trees can be intense during the prolonged dry season. Vulnerability to embolism consistently changed with ontogeny and varied with tree species' stature (maximum height): mature individuals of larger species displayed increased vulnerability, whereas smaller species displayed unchanging or even increased resistance at the mature stage. The ability to change drought-resistance strategies (vulnerability to embolism) through ontogeny was positively correlated with ontogenetic increase in iWUE. Ecologically, overstory trees appear to shift from being hydraulically drought resilient to persisting under dry soil surface layer conditions to being more likely physiological drought avoiders as adults when their roots reach wetter and deeper soil layers.

Keywords Embolism resistance · $\delta^{13}C$ · Stable isotope · Hydrological niche segregation · Ontogenetic shift · Phenotypic plasticity · Amazon rainforest · Water-use efficiency

Communicated by Daniel Potts.

✉ Mauro Brum
maurobrumjr@gmail.com

1 Department of Ecology and Evolutionary Biology, and department of Environmental Science, University of Arizona, Tucson, AZ, USA

2 Center for Tropical Research, Institute of the Environment and Sustainability, University of California-Los Angeles, Los Angeles, CA 90095, USA

3 Embrapa Amazônia Oriental, NAPT Médio Amazonas, Santarém, PA, Brazil

4 Laboratory of Wood Technology and Bioproducts, Federal University of Western Para, Santarem, PA, Brazil

5 Universidade Federal do Pará, Instituto de Ciência Biológicas, Belém, PA, Brazil

6 Applied Ecology Laboratory, Interdisciplinary and Intercultural Training Institute, Federal University of Western Pará, Santarém, PA, Brazil

7 Universidade Federal do Oeste do Pará, Instituto de Ciências e Tecnologia das Águas, Santarém, PA, Brazil

8 Centro de Energia Nuclear na Agricultura (CENA), Universidade de São Paulo (USP), Piracicaba, SP, Brazil

9 Embrapa Amazônia Oriental, Laboratório de Botânica, Belém, PA, Brazil

10 Department of Forestry, Michigan State University, East Lansing, MI 48824, USA

11 Institute of Engineering and Geosciences, Federal University of Western Para, Santarem, PA, Brazil

12 Department of Plant Biology, Institute of Biology, Universidade Estadual de Campinas (UNICAMP), CP 6109, Campinas, SP 13083-970, Brazil

Introduction

Plants face intermittent water stress, which affects species distribution and carbon (C)-allocation strategies in tropical forests (Engelbrecht et al. 2007; Esquivel-Muelbert et al. 2016, 2020; Signori-Müller et al. 2021). In the Amazon forest, trees have evolved various hydraulic strategies critical for determining drought responses and resilience to intermittent water stress (Cosme et al. 2017; Barros et al. 2019; Fontes et al. 2020; Garcia et al. 2021). Large trees may be affected disproportionately by drought (Nepstad et al. 2007; Rowland et al. 2015; McDowell et al. 2018), but other studies suggest that tall Amazon forests are less sensitive to precipitation variability (Giardina et al. 2018), and larger trees have greater access to deeper soil water (Brum et al. 2019). However, insufficient knowledge exists regarding hydraulic strategies and C-allocation constraints across tree sizes, including adult stature and ontogenetic variation (Rowland et al. 2015; Bittencourt et al. 2020).

Environmental filters differentially shape both patterns of tree physiological performance and carbon allocation across ontogenetic stages (Lasky et al. 2015; Brienen et al. 2017; Dayrell et al. 2018; Henn and Damschen 2021). These developmental patterns are often associated with ontogenetic shifts in traits—which are the result of plasticity mechanisms that confer to a genotype the ability to produce different phenotypes depending upon the growing environment—and can be observed among any of the traits affecting the coordination of whole-plant physiological function and performance (Weiner 2004; Lasky et al. 2015; Power et al. 2019). Vertical forest profiles impose contrasting gradients in light, vapor pressure deficit (VPD), and CO_2 concentration, potentially driving ontogenetic shifts within a tree's lifespan, which might be described as strategies to respond to the changing conditions experienced as the tree becomes larger (Thomas & Bazzaz 1999; Sterck et al. 2013; Stark et al. 2012; Tang & Dubayah 2017). In the seasonal Amazon forest, photosynthetic traits and leaf area distribution are integrally connected to tree size distribution (Domingues et al. 2005; Stark et al. 2012; Smith et al. 2019), and the aboveground vertical structure is related to the effective rooting depth at which tree water uptake occurs (Markewitz et al. 2010). If this above-belowground integration drives the drought tolerance-avoidance spectrum within the community (Brum et al. 2019), young trees of dominant overstory species are expected to be shallow rooted because of constraints in biomass allocation due to light interception (Thomas & Bazzaz 1999; Santos et al. 2018). During this stage, trees may require a high degree of drought tolerance to survive in a dense understory environment, where competition for space, light, and shallow soil water among smaller trees can be intense during the prolonged dry season (Rice et al. 2004; Stark et al. 2012; Brum et al. 2019).

Trees that face repeated droughts may need to adjust their hydraulic system and maintain coordination between water loss and C-metabolism (Brodribb et al. 2002; Oliveira et al. 2021). Xylem embolism resistance, estimated by P50 and P88, is crucial for determining drought resistance in response to water stress (Sperry et al. 2002; Meinzer et al. 2009; Meinzer and McCulloh 2013) as it influences the safety range of the water potential for water transport without embolism failure (Choat et al. 2012; Anderegg et al. 2016). Regulation of stomatal conductance can prevent embolism formation by maintaining the water potential within a safe hydraulic range (Brodribb et al. 2002; Sperry et al. 2002). The degree of hydraulic conservatism that depending on stomatal regulation—have different long-term impacts on intrinsic water-use efficiency (iWUE), the ratio of photosynthesis to water loss (Farquhar and Lloyd 1993; Cernusak et al. 2001; McCaroll and Loader 2004). Alignment of iWUE with stomatal regulation and drought-resistance traits in tropical Amazon forests remains relatively unknown (Garcia et al. 2021). One way to estimate iWUE is to analyze the stable carbon isotope ratio ($\boldsymbol{\delta^{13}C}$; ‰) of leaf tissue, with heavier ^{13}C being discriminated by RuBisCO when stomata are less controlled, as indicated by low iWUE (McCaroll and Loader 2004). However, the estimation of iWUE from $\delta^{13}C$ is affected by ontogenetic shifts over differences in tree height, which impacts drought and hydraulic patch resistance, and the CO_2 concentration and $\delta^{13}C$ signature across the vertical forest profile (Vadeboncoeur et al. 2020; McDowell et al. 2011; Brienen et al. 2017; Mathias & Thomas 2021).

Our study aimed to investigate how Amazon tree species at different heights cope with the hydrological and light niche axes across their ontogeny in the vertical forest profile. We tested the niche acclimation hypothesis that there is a gradient in ontogenetic shifts in embolism resistance and iWUE, with greater differences occurring in overstory species (Fig. 1). Overstory species would exhibit higher ontogenetic shifts in their tolerance to xylem embolism, with saplings displaying more drought-resistant traits than mature individuals. In contrast, understory species would exhibit fewer ontogenetic shifts in their tolerance to xylem embolism. Both mature and sapling understory species have higher tolerance to xylem embolism. Similarly, tree saplings have higher iWUE than their mature conspecifics, with this ontogenetic shift in iWUE being more pronounced in overstory species than in understory species, likely because of changes in the water and light environment.

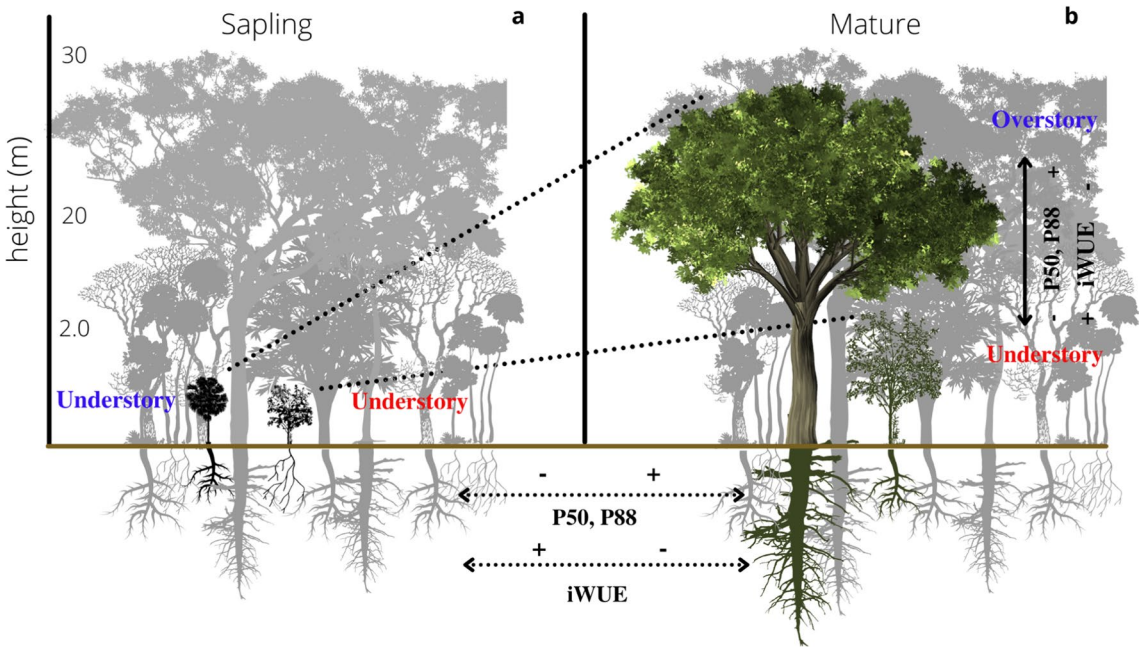

Fig. 1 The niche acclimation hypothesis under investigation in this study. We explored the gradient in ontogenetic shifts in embolism resistance (P50, P88) and intrinsic water-use efficiency (iWUE) across species and forest strata. We expected that overstory species exhibit greater ontogenetic differences in their tolerance to xylem embolism, with saplings displaying more drought-resistant traits than mature individuals. In contrast, understory species exhibit fewer ontogenetic shifts in their tolerance to xylem embolism, with both mature and sapling individuals displaying higher tolerance levels. We also expected a higher iWUE in tree saplings than in mature conspecifics, with overstory species showing a more pronounced ontogenetic shift in iWUE compared to understory species, possibly due to differences in water and light availability

Methods

Site description

Our study was conducted at km67 (the LBA-ECO/Ameriflux tower site) in Tapajós National Forest, Brazil (54° 96′ W and 2° 86′ S). The forest is Forest is predominantly evergreen, with a mean height of ~ 40–45 m in the overstory layer and a dense understory (Smith et al. 2019). The area is located in the Barreiras Formation, characterized by a deep, well-drained Dystrophic Yellow Latosol soil with a high clay fraction (Oliveira-Junior & Correa 2001). Mean annual temperature is 25 °C and annual precipitation of 2037 mm between 1998 and 2019. The climate exhibits strong seasonality, during which the monthly precipitation drops below 100 mm (Restrepo-Coupe et al. 2016), and shallow soil water presents a significant decrease from August to November (Ivanov et al. 2016).

Species selection

Our study included eight dominant species categorized by their distribution in the forest based on stems with a diameter at breast height (DBH) of ≥ 10 cm, as identified in previous forest inventories (Pyle et al. 2009, updated by Longo 2013; see Table 1). We added two small understory species (mostly with stems < 10 cm DBH), which were not originally included in the inventory (Table 1). Based on the maximum height achieved locally (H_{max}, calculated as the 95th percentile height), we classified the species as overstory (H_{max} > 35 m), midstory (H_{max} > 15-35 m), or understory (H_{max} < 10 m) (Smith et al. 2019).

In 2019, we evaluated iWUE and xylem hydraulic traits of trees by tagging and sampling them in the field. To ensure accurate sampling of small saplings and adult trees, a taxonomist and parataxonomist from the Brazilian Agricultural Research Corporation (EMBRAPA-Belém) identified all sampled individuals. We defined saplings as individual trees < 1 cm DBH of each target species, and only sampled those located in the deep-shaded understory, excluding forest clearings. We measured the diameter (30 cm from the ground) and height of saplings. The data and samples of mature individual trees (> 10 cm DBH) were obtained from previous work published in Brum et al. (2019). The sample sizes and ontogenetic category are listed in Table S1. Branch samples were obtained using climbing, ladders, or pole pruners, depending on accessibility (Table 1). Owing to the challenge of accessing the top layer, most samples from mature individuals were obtained from the lower and intermediary overstory layers. Upon arrival at the base camp

Table 1 Biological and structural attributes of the species studied at the Tapajós Forest km 67 LBA study area, Brazil

Species*	Family	H_{max} (m)	Canopy position	Basal area (m^2/ha)	Abundance (ind/ha)
Manilkara elata (Allemão ex Miq.) Monach.[1]	Sapotaceae	41.8	Overstory	2.19	10.5
Erisma uncinatum Warm	Vochysiaceae	48.8	Overstory	3.64	11.0
Chamaecrista scleroxylon (Ducke) H.S.Irwin and Barneby[2]	Leguminosae	35.2	Overstory	2.01	15.5
Protium apiculatum Swart	Burseraceae	25.8	Midstory	0.65	24.3
Coussarea paniculata (Vahl) Standl.[3]	Rubiaceae	17.1	Midstory	1.48	92.5
Miconia sp.	Melastomataceae	17.2	Midstory	0.08	2.5
Amphirrhox longifolia (A.St.-Hil.) Spreng	Violaceae	5.5	Understory	0.35	908
Rinorea pubiflora (Benth.) Sprague and Sandwith	Violaceae	4.3	Understory	2.45	3104

Values for basal area and abundance represent average across a 4-ha survey area of all trees larger than 10 cm in diameter at breast height. Two understory species (*A. longifolia* and *R. pubiflora*) were recorded in five 0.05-ha plots. Species in the table are listed in the order that has the deepest rooted species at the top, and the shallowest rooted species at the bottom, as determined in Brum et al. (2019). The maximum height attained (H_{max}, *m*) per species was calculated as the 95th percentile of the distribution of tree heights**. For the understory species, H_{max} was calculated from direct height measurements

*Species names updated since Brum et al. (2019)

**Individual tree height (*H*) was estimated by applying a site-derived allometric model using *H* and *dbh* as predictors; a total of 7724 individual trees had their *dbh* (cm) and height (m) measured in the field using clinometers were employed to build the model:

$H = 96.52\ [1 - \exp(-0.02636\ \mathrm{DBH}^{0.6682})]$, as described in Longo et al. (2016)

[1]Identified in Km 67 species inventory as *Manilkara huberi*, but updated after a new floristic inventory (Herbario IAN, EMBRAPA Belem) as accepted name *Manilkara elata*

[2]Identified in Km 67 species inventory as *Chamaecrista xinguensis* but updated after a new floristic inventory (Herbario IAN, EMBRAPA Belem) as accepted name *Chamaecrista scleroxylon*

[3]Identified in Km 67 species inventory as *Coussarea albescens* but updated after a new floristic inventory (Herbario IAN, EMBRAPA Belem) as accepted name *Coussarea paniculata*

(~20 km from the sampling site), three to five leaves per tree individual were refrigerated, dried at 65 °C for 36 h, and frozen until transported to the University of Campinas, São Paulo, Brazil.

Tolerance to xylem embolism

To evaluate the drought-resistance strategies between the two ontogenetic categories, we measured the vulnerability of xylem embolism to obtain the P50 and P88 (MPa) in sapling and in conspecific mature species. We used the pneumatic method to measure the xylem embolism resistance for each branch (Pereira et al. 2016; 2020). The loss of hydraulic conductivity is estimated based on the increase in air volume inside the wood caused by embolism formation, as the branch loses water according to the bench method (Sperry et al. 1988). Here, the air volume was estimated from the air discharge from the cut end of the branch into a vacuum reservoir of known volume during 2.5 min. To equilibrate the leaf and wood xylem water potential, we bagged the branches for 1 h before each air discharge measurement. Immediately after the air discharge was measured, we detached a leaf sample from the branch and measured the leaf water potential using a pressure chamber (PMS 1000; PMS Instruments Co). For every leaf removed from the branch, we used a wood glue to close the branch point and avoid leakage of air within the branch for the next air discharge measurement (Bittencourt et al. 2018). The drought embolism resistance was given by the increase in air discharge (PAD—percentage of air discharge) with the reduction in xylem water potential for each branch segment. Here, we include the data for each branch including replicates from the same species and ontogenetic class and fitted a sigmoid curve to measurements, where P50 and slope (b) are the fitted parameters (Pammenter and Vander Willigen 1998) is predicted from the fitted model as follows:

$$\mathrm{PAD} = \frac{100}{(1 + \exp(a.(\Psi - P50))}, \quad (1)$$

where PAD is the percentage of air discharged (%), a is the fitted slope, and Ψ is xylem water potential when PAD is equal to 50% (MPa).

Determining the intrinsic water-use efficiency (iWUE)

We used $\delta^{13}C$ (‰) in the leaf bulk to calculate iWUE. The $\delta^{13}C$ discrimination is related to the ratio of mesophyll (c_i; ppm) to atmospheric CO_2 concentrations (c_a; ppm) and

reflects the transpiration-photosynthesis balance (Farquhar et al. 1982). A higher c_i/c_a ratio leads to less controlled stomatal conductance, causing RuBisCO to strongly discriminate against $\delta^{13}C$, decreasing iWUE. In contrast, a low $c_i{:}c_a$ ratio leads to higher stomatal control and a drop in internal c_i, resulting in less RuBisCO discrimination against ^{13}C, increasing iWUE (McCarrol & Loader 2004). To obtain leaf $\delta^{13}C$, we ground dried leaves into a fine powder using the Geno/Grinder® SPEX SamplePrep. Samples were then aluminum encapsulated, weighed in a micro-analytical (1–2 mg) balance, and sent to the Laboratory of Isotope Ecology, University of São Paulo. Additional information regarding the determination of $\delta^{13}C$ is available in the supplementary material.

To account for the potential effects of tree height and soil respiration on water-use efficiency, using the $^{13}C{:}^{12}C$ ratio (Medina & Minchin 1980; Sternberg et al. 1989; Brienen et al. 2017; Vadeboncoeur et al. 2020), we estimated the expected $\delta^{13}C_a$ amplitude in the aboveground vertical forest profile (62, 50, 39, 29, 20, 10, 3, and 1 m above the surface) (Figures S1 and S2). We used long-term measurements of atmospheric CO_2 concentrations across a height profile at the LBA km67 flux tower (Restrepo-Coupe et al. 2013; 2016), and calculated the average daily cycle of all available hourly measurements from 2001 to 2020 to obtain the overall vertical CO_2 concentration gradient at the site (Figure S2-A and C). We estimated the $\delta^{13}C$ of air samples using an equation based on the 'Keeling plot' and a model previously fitted to a primary forest in our study site ($\delta^{13}C = 6821.8 * 1/CO_2 - 26.96$; $r^2 = 0.97$; Figure S3; Ometto et al. 2002). We derived a nonlinear model between the daytime average c_a and estimated $\delta^{13}C$ as a function of tower height (Figure S2B–D), allowing us to predict atmospheric $\delta^{13}C$ ($r^2 = 0.97$; $p < 0.001$; RMSD = 0.09‰) and c_a ($r^2 = 0.97$; $p < 0.001$; RMSD = 18 ppm) (eqS3 and eqS4; Figure S4).

We estimated the height of the trees sampled in the field using height-diameter allometry derived for trees at our research site (Longo et al. 2016; Table S1). We measured the individual sapling heights in the field using measurement tapping. We predicted the average atmospheric $\delta^{13}C$ and c_a using equations S3 and S4, based on the specific vertical forest atmosphere where the leaves grew. We calculated iWUE as follows:

$$\text{iWUE} = \frac{ca(b + \delta 13\text{Cp} - \delta 13\text{Ca})}{1.6(b - x)}, \quad (2)$$

where c_a is the CO_2 atmospheric concentration, $\delta^{13}C_a$ is the C isotope ratio of the atmosphere, $\delta^{13}C_p$ is the measured isotope ratio of the leaf tissue, x is the diffusive fractionation coefficient against $^{13}CO_2$ (4.4‰), b is the carboxylation fractionation coefficient of $^{13}CO_2$ by RuBisCO (27‰), and 1.6 is the ratio of diffusion rates of water vapor to CO_2. A correction term was applied for the bulk of $\delta^{13}C_p$, as it was slightly depleted relative to the $\delta^{13}C$ from the sugar substrate in which leaf compounds were produced, with an average of 5.1‰ added to each value of $\delta^{13}C_p$ before calculating the iWUE. This correction was needed because a non-corrected $\delta^{13}C_p$ derived a negative iWUE (Figure S5).

Data analysis

We compared the P50, P88, and slope from the vulnerability curves of saplings and mature trees, independent of species, using a one-way fixed effect to test for statistical differences. Differences in the homogeneity of variances between the groups were calculated using Levene's test to measure trait variation. We used a two-way fixed effect to test for differences in iWUE between saplings and mature trees as well as their interaction with forest strata where the species grows in the mature stage. Another two-way fixed effect was used to test for species-specific differences in iWUE between the saplings and mature trees. R software was used for all tests (R Core Team 2017), with the generalized least square model (GLS) function utilized from *nlme* package (Pinheiro et al. 2018), which allows for correlated errors and unequal variance in the fixed terms. We compared the models using the ANOVA function from the *car* package, which reports the likelihood-ratio Chi Square (X^2) and gives the effect size and p value for the fitted models (Fox and Weisberg 2011). We conducted a post hoc test using the *emmeans* package to estimate the mean contrast for specific factors or factor combinations (Lenth 2019). Pairwise comparisons were used to identify specific mean differences, and p values were adjusted using the Tukey method.

Two indices of phenotypic plasticity were used to describe the ontogenetic shift between saplings and mature conspecific species for P50, P88, and iWUE. The first index, the coefficient of variation (CV = SD/mean), examines the relative variability of traits within species, including sapling and mature data (Power et al. 2019). The second index, the ontogenetic difference (OD), determined the absolute difference in P50 and P88 between saplings and mature trees. Positive OD indicated increased drought resistance to xylem embolism in the mature stage, whereas negative values indicated higher iWUE in saplings. We used CV and OD for P50, P88, and iWUE as functions of maximum tree height estimated from DBH measurements, which is a proxy for species life history related to height and rooting depth across the understory–overstory gradient in the mature stage (Brum et al. 2019). Finally, we calculated Pearson correlations between the indices of phenotypic plasticity and variables. We also used a multiple generalized linear model (GLM) to evaluate the effects of interaction between height and P50 on the average iWUE. P88 was not used to avoid multicollinearity with the P50. Standardized coefficients (β)

were compared to assess the relative influence of independent variables on iWUE.

Results

Drought-resistance strategies in the vertical eco-hydro-light environment

The P50, P88, and shape of the vulnerability curves varied according to tree ontogeny for some species, but not for others (Fig. 2). However, when all plants were included, the average P50, P88, and slope of the vulnerability curve did not vary between the saplings and mature trees (GLS; $p > 0.05$). Although the mature individuals exhibited higher variance in P50 compared to saplings (Levene test, $p < 0.05$), the variance in P88 and slope were similar between the two stages (Levene test, $p > 0.05$; Fig. 3). On average, for saplings, P50, P88, and the slope were −2.94 MPa (± 0.36), −4.86 MPa (± 0.80), and 1.12% MPa^{-1} (± 0.30), respectively (± standard deviation). Mature trees exhibited an average P50 of − 3.18 MPa (± 1.13), P88 of − 4.79 MPa (± 1.43), and slope of 1.52%.MPa^{-1} (± 0.82).

The overstory species *E. uncinatum* and *M. elata* exhibited higher embolism resistance in the sapling stage, with a negative OD, implying an increase in P50 and P88 from the sapling to the mature stages. Conversely, midstory *C. paniculata* and *Miconia* sp. showed more negative P50 and P88 in the mature stage, whereas other understory species, including *P. apiculatum*, had similar P50 and P88 in both the mature and sapling stages (Fig. 4). The coefficient of variation for P50 and P88 was positively correlated with the estimated maximum height (H_{max}) at maturity, with 46% ($p = 0.06$) and 52% ($p = 0.03$), respectively. But there was

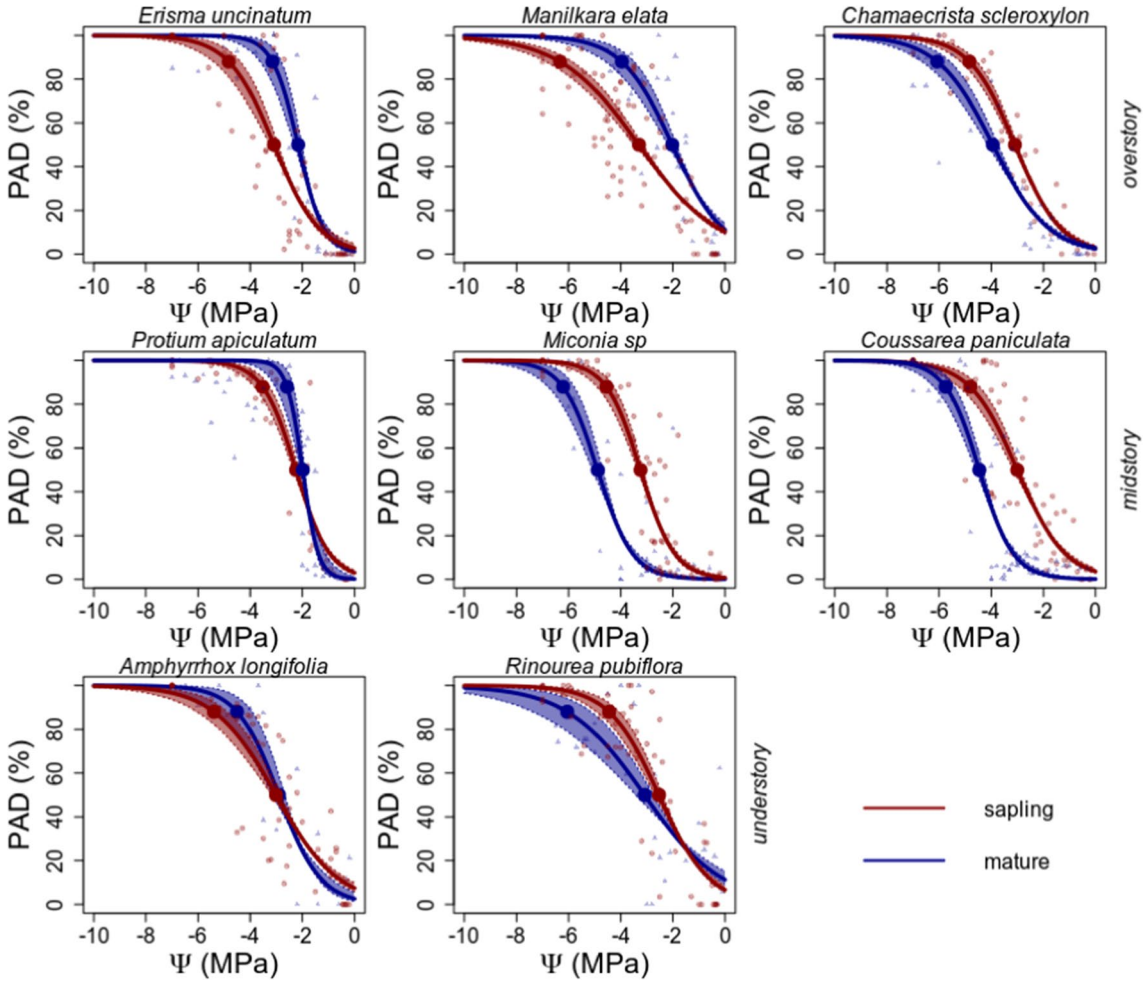

Fig. 2 Hydraulic vulnerability curves (PAD—percentage of air discharge vs. stem water potential) for different species and ontogeny class from seasonal Amazon in Tapajós Forest, Belterra-PA, Brazil. The thicker lines denote the sigmoid curve to the data, and the shadow area shows the standard error of the coefficient estimates given by the nonlinear model function (*nls* function in R). The red color represents the data from saplings and blue the mature individuals. From top to bottom panels, species are sorted by their position in the canopy: over to mid to understory

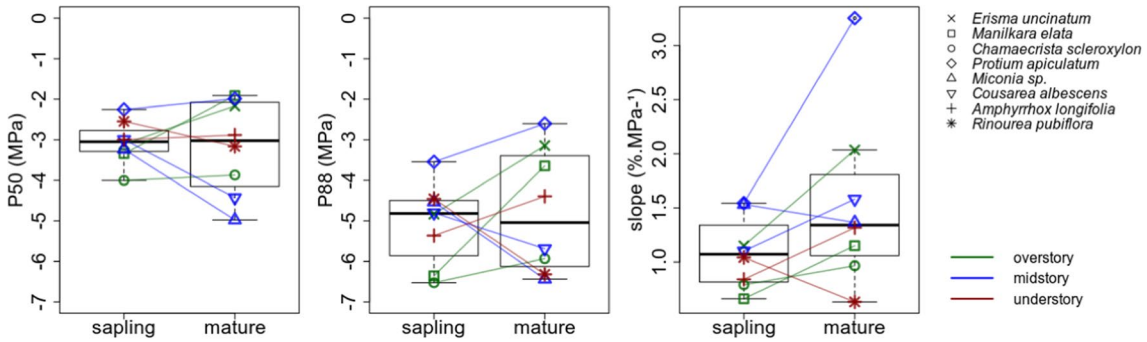

Fig. 3 Box plot of the water potential (MPa) where plant loss 50% (P50) and 88% (P88) for sapling and mature individuals. Each line connects the P50 and P88 value between conspecific sapling and mature individuals

no correlation between H_{max} and the CV slope ($R = 0.17$; $p = 0.54$). The absolute difference in P50 and P88 between saplings and mature trees was negatively correlated with H_{max}, with a 66% and 69% decrease, respectively (Pearson correlation, $p < 0.05$); however, H_{max} was not related to the ontogenetic difference in slope from the vulnerability curve ($R = 0.16$; $p = 0.54$).

Intrinsic water-use efficiency (iWUE)

Mature trees had a higher iWUE than saplings, with an average of 99 ± 39 µmol/mol, which was 17.2 µmol/mol higher (GLS, $F = 9.12$; $p < 0.01$). The ontogenetic stage and forest strata did not significantly explain the variance in leaf iWUE (GLS, $F = 0.54$; $p = 0.58$), and there were no differences in iWUE between mature and sapling trees in the overstory, midstory, and understory (Post-HocTukey; $p > 0.05$). Four species showed a positive change in iWUE from sapling to mature stage, namely *E. uncinatum* and *M. elata* in the overstory, *C. paniculata* in the midstory, and *R. pubiflora* in the understory. Only *A. longifolia* showed a significant increase in iWUE in the sapling stage compared to mature individuals, among the three species that had a higher iWUE in saplings than in mature individuals (Fig. 5).

Tree height had a significant positive effect on rates of the mean leaf iWUE (GLM; $X^2 = 18.30$; $p < 0.001$), regardless of the ontogenetic stage. However, the P50 and vulnerability slope were not significantly correlated with iWUE ($p < 0.05$). The interaction between P50 and tree height had a significant effect on leaf iWUE rates (GLM; $X^2 = 7.40$; $p < 0.05$). The predicted iWUE rates had an intercept of − 43.64 (std error ± 47.54; $p = 0.37$) and a strong positive effect of tree height (slope = 7.13 ± 2.04; $p = 0.004$), while P50 had a negative effect (slope = -41.96 ± 16.13; $p = 0.02$), and the interaction between P50 and tree height had a positive effect (slope = 2.18 ± 0.80; $p = 0.01$). The iWUE pattern varied with tree size at different P50 values (Fig. 6). The absolute ontogenetic difference in iWUE between mature and sapling trees was positively correlated with the coefficient of variation of P50 ($R = 0.86$; $p < 0.05$; Fig. 7) but not with the absolute ontogenetic difference in P50 ($R = -0.11$; $p = 0.68$; not shown).

Discussion

As expected, we observed changes in drought-resistance strategies (P50 and P88) from the sapling to mature stages in the two largest overstory species (*M. elata* and *E. uncinatum*); these species were less vulnerable to xylem cavitation in the sapling stage. Our findings generally supported our hypothesis; for instance, the understory species (*A. longifolia* and *R. pubiflora*) had less hydraulic variability during the ontogenetic stages. Species with canopy niches falling between these extremes showed greater variability, and there were no differences between saplings and mature conspecifics in the overstory *C. scleroxylon* and midstory *P. apiculatum*. In contrast, two midstory species (*C. paniculata* and *Miconia* sp.) displayed a much higher resistance to xylem embolism in the mature stage. These patterns indicate that the variations in drought-resistance strategies between mature trees and seedlings are strongly influenced by the intrinsic characteristics of the species, while for some genotypes, the mechanisms of phenotypic plasticity exist, and for others they do not (Fig. 4).

Contrary to our hypothesis, we did not find higher iWUE in saplings than in conspecific mature individuals, nor was this effect more pronounced in understory species. Instead, we observed that for four species, mature individuals had significantly higher iWUE than saplings, regardless of the forest stratum. Instead of higher water-use efficiency in the understory, we found that iWUE was related to xylem embolism resistance and tree height, with these factors leading to contrasting iWUE patterns in mature and small sapling trees (Fig. 6). Our GLM model suggests that iWUE increases with stature for individuals with low embolism

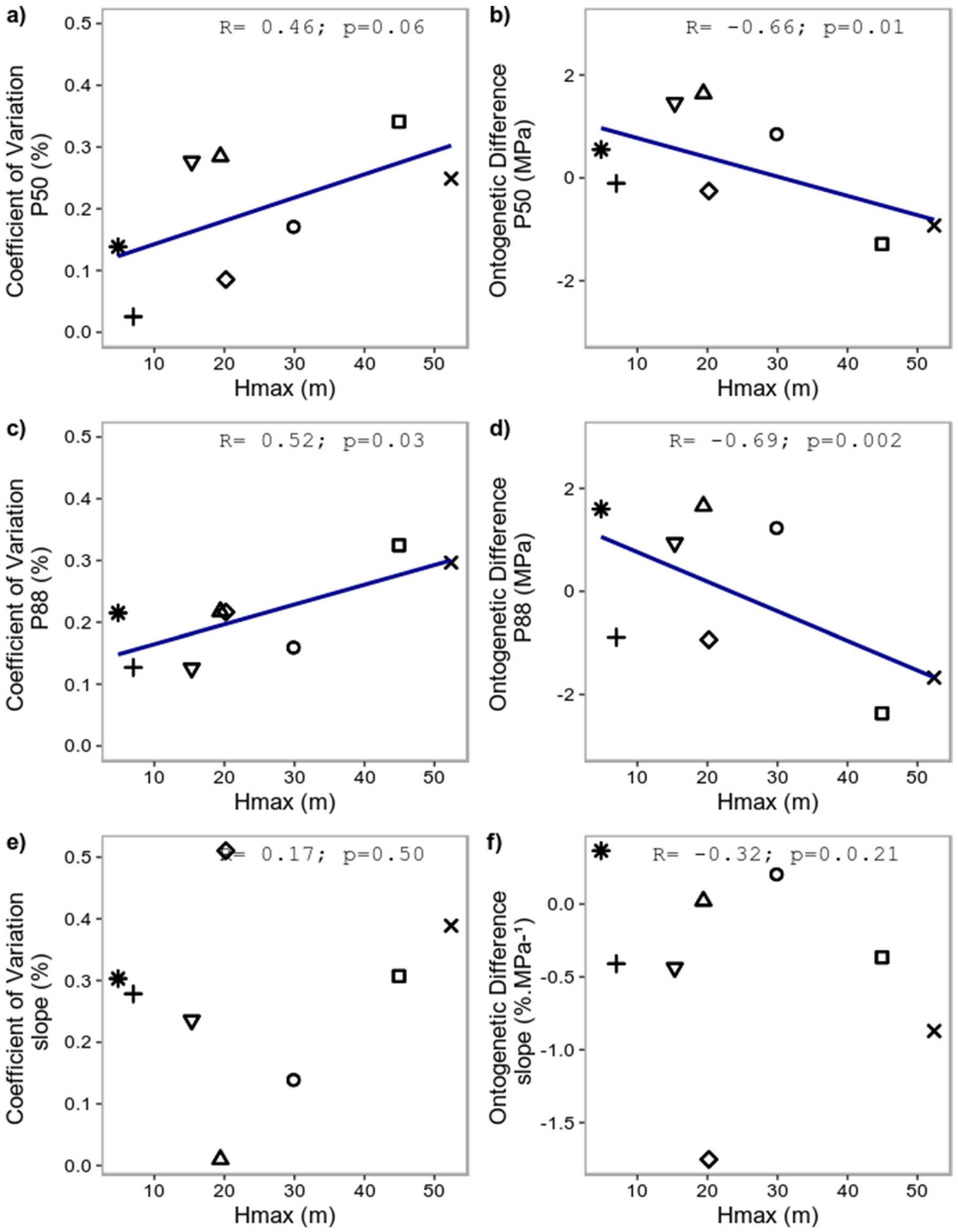

Fig. 4 Correlation between coefficient of variation (CV; **a, c, e**) or ontogenetic difference (OD; **b, d, f**) of the sapling and mature P50 and P88 and the maximum height that mature tree species reach in our samples. Symbols represent a single individual in the sample, same as shown in Fig. 2

resilience, whereas iWUE decreases with stature among individuals with high embolism resilience. Correspondingly, the direction of ontogenetic shifts in iWUE was related to the species' ability to shift drought-resistance strategies (CV P50; Fig. 7) throughout its life, suggesting that ontogenetic changes in drought resistance may result in the maximization of mature-stage iWUE (described in the next section). Our findings support the hydrological niche acclimation

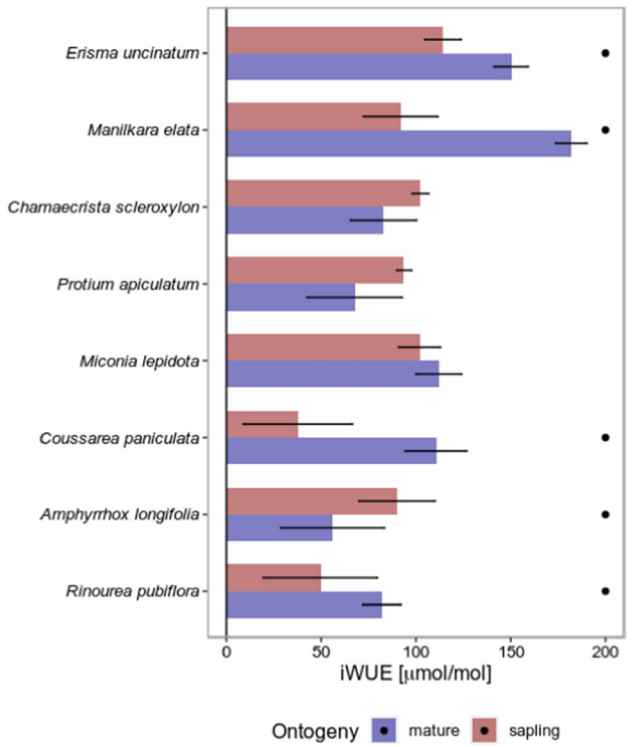

Fig. 5 The mean (column) and standard deviation (bar) of the bulk estimated intrinsic water-use efficiency (iWUE) calculated by the $\delta^{13}C$ method. Each black point represents that the mean difference was significant from mature to sapling stages (PostHoc test, $p < 0.05$). Species are sorted from top to bottom by the position in the canopy from overstory (*E.uncinatum, M. elata, C. scleroxylon*), to midstory (*P. apiculatum, M. lepidota, C. paniculata*) to understory species (*A. longifolia, R. pubiflora*)

hypothesis, demonstrating the need for ontogenetic adjustments in plant hydraulic systems to maintain coordination with carbon metabolism in tree species exposed to repeated drought events across hydrological niches in the seasonal Amazon forests.

Acclimation of xylem hydraulic vulnerability

Variations in below- and aboveground water availability and spatial light distribution (Domingues et al. 2005; Ivanov et al. 2012; Stark et al. 2012; Brum et al. 2019) induced local hydrological niche acclimation and ontogenetic shifts in tree traits in a seasonal Amazon forest. Our study found that maximum tree height (H_{max}) can predict variability in embolism resistance (P50 and P88), but absolute ontogenetic differences vary among species (Fig. 3, 4), which is consistent with other studies in the Easter Amazon forest (Rowland et al. 2015; Bittencourt et al. 2020). We discovered that the dominant overstory species in the seasonal forest exhibited local physiological plasticity as saplings with shallow roots. These change patterns require high embolism resistance for survival in a water-limited understory (Rice et al. 2004; Fonti et al. 2010; Brum et al. 2019) and emphasized the importance of root development in deeper soil to buffer shallow soil drought effects (Silvertown et al. 2015; Nardini et al. 2016), suggesting that juvenile and small-statured trees converge on traits common to understory regeneration niches but not on traits important for mature stages (Thomas & Bazzaz 1999; Reich 2000). Thus, ontogenetic shifts in hydraulic strategies may respond to ontogeny-dependent filters (Dayrell et al. 2018), indicating that tree hydraulic trait

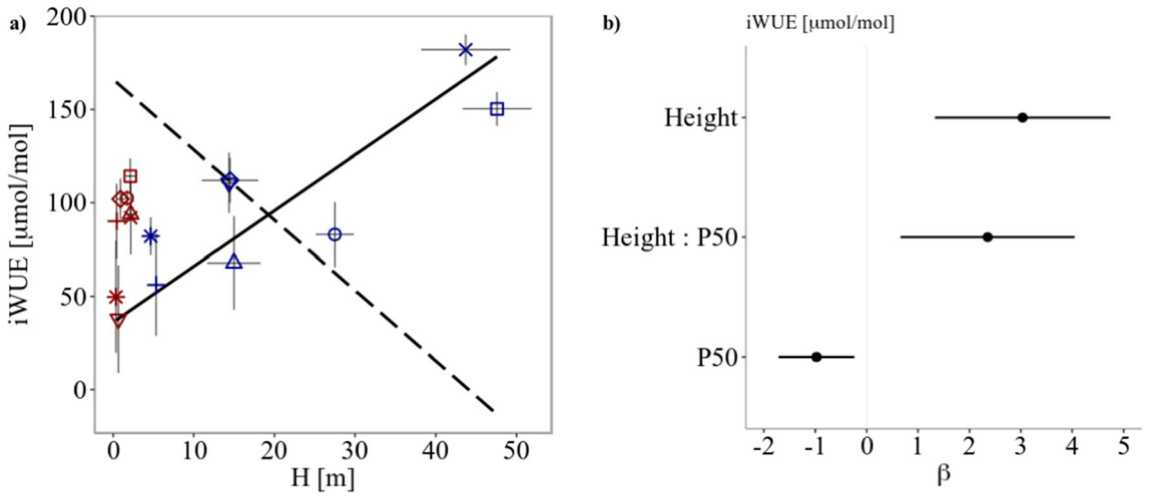

Fig. 6 **a** The mean intrinsic water-use efficiency (iWUE) as a function of the height (*H*) of sampled trees including average mature (blue) and average sapling (red) for each species (symbols described in Fig. 2). The lines represent the fitted iWUE values derived from the generalized linear model (GLM; iWUE ~ H + P50 + H:P50), the continuous line represents the fitted values when the P50 is − 2 MPa, and the dashed line represent the model when the P50 is − 5 MPa. **b** Standardized coefficients (β) and confidence intervals resulting from the GLM analysis. Number of standard deviations (SDs) an iWUE will change per SD increase in either tree height or P50

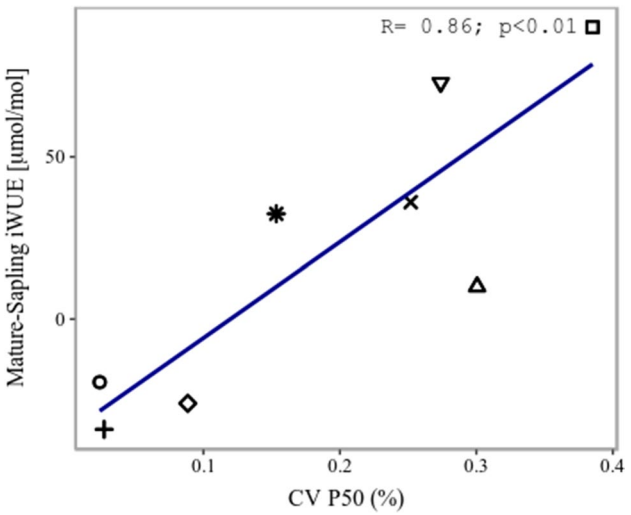

Fig. 7 Correlation between the mean absolute difference between the intrinsic water-use efficiency (iWUE) of leaves of mature and sapling stages and the coefficient of variation (CV) of the sapling and mature P50 (CV P50; %) individuals. Symbols represent the species included in this study as identified in Fig. 2

evolution is the result of natural selection pressures arrayed across all stages of tree life history, shifting from drought tolerance in the early regeneration niche to drought avoidance in the later persistence of larger overstory trees in the seasonal Amazon forest.

With the roots of overstory trees growing into deeper soil strata with low variation in soil moisture across the season, trees may be expected to maximize water transport to greater heights with higher hydraulic conductivity (Liu et al. 2019; Olson et al. 2018; Bittencourt et al. 2020; Kotowska et al. 2021). This pattern may be expected even if taller trees are more exposed to higher radiation loads and drier atmospheric conditions (higher vapor pressure deficit, VPD) in the overstory layer, and are physiologically more vulnerable to water stress (Mencuccini 2003; McDowell & Allen 2015; Liu et al. 2019). Interestingly, understory and midstory species with predominantly shallow roots in the mature stage did not display ontogenetic shifts in P50 and P88 or a higher tolerance to xylem embolism in the mature stage. These species do not reach the overstory stage as mature individuals and, thus, may be buffered from extreme VPD conditions by occurring in a more humid understory. In addition to supporting survival in the absence of ontogenetic trait shifts, these species tolerate strong decreases in leaf water potential driven by seasonal reductions in shallow soil water availability in the Tapajós forest, in addition to having a high xylem embolism tolerance (Brum et al. 2019). Our results point to an important mechanism related to the drought resistance–avoidance axis: increase in access to soil moisture deeper in the soil as trees grow taller is an important driver of ontogenetic shifts of xylem embolism resistance in a seasonal tropical forest. A tree's life history strategy also plays an important role, that is, smaller-stature species follow 'understory' strategies across ontogenetic stages (Fernández-de-Uña et al. 2023). As the decrease in embolism resistance with tree size is highly dependent on the combination of genera analyzed in the Amazon forest (Rowland et al. 2015; Bittencourt et al. 2020), and we suggest that this pattern may co-vary with ontogenetic changes in the root water uptake. Here, we hypothesized that drought-tolerant taxa that are disproportionately widespread across precipitation gradients in the Amazon forest (Esquivel-Muelbert et al. 2016, 2020; Tavares et al. 2023) might have more ontogenetic hydrological acclimation abilities than wet-affiliated species, with a typically restricted distribution to wetter places across the basin. We also noted that the role of changing soil moisture access in ontogenetic shifts may be critically affected by soil hydrology, with differences associated with the average depth of soil water tables (e.g., very shallow vs. deep) and their fluctuations, a major environmental gradient in the Amazon across regional differences in rainfall (Oliveira et al. 2019; Costa et al. 2023).

Acclimation in iWUE

Our study aimed to examine the associations between tree height, rooting depth, and iWUE (Vadeboncoeur et al. 2020). Unexpectedly, iWUE was positively and strongly correlated with tree height (70%). Some evidence suggests that larger tree species with greater access to deeper water sources (in this study, tall trees) may exhibit higher iWUE due to a higher degree of stomatal regulation, that is, more isohydric behavior (Ding et al. 2021). We also found that small trees with higher resistance to xylem embolism had higher iWUE, whereas vulnerable species had lower iWUE (Fig. 6; compare the dashed high tolerance and solid low tolerance lines). Interestingly, changes in iWUE co-varied with changes in tree xylem resistance to drought, which are associated with an ontogenetic shift in tree physiological performance related to water availability (Briennen et al. 2017) and with light gradients over canopy strata (Vadeboncoeur et al. 2020). Moreover, the direction of the ontogenetic shift in iWUE was strongly linked to the ability of the species to alter drought-resistance strategies (CV P50 covariation with H_{max}) (Fig. 7). This suggests that changes in drought resistance and avoidance shifts were associated with the maximization of iWUE in the mature stage of overstory trees.

At Tapajos, larger overstory trees have greater control over the minimal water potential during water stress, despite having greater access to deep water sources (Brum et al. 2019). Small trees and species with a higher tolerance to xylem embolism also had higher iWUE. Previous studies have shown that height affects leaf isotope discrimination

in Tapajos (Ometto et al. 2002; Domingues et al. 2005), and we propose that this pattern can be attributed to (1) an increase in light availability in the overstory layer, leading to a higher maximum photosynthetic rate (Thomas and Bazzaz 1999; Rijkers et al. 2000; Domingues et al. 2005), which results in increased carbon assimilation in the overstory layer and (2) an increase in stomatal control to avoid decreases in leaf water potential and minimize xylem cavitation in larger overstory trees with less negative P50 in the mature stage (Fig. 4; Santos et al. 2018; Garcia et al. 2021; Ding et al. 2021). These physiological performance factors have contrasting net effects on iWUE in larger and smaller trees by increasing assimilation more than stomatal conductance in sunlight-exposed leaves, which predominantly occurs in the canopy (Zhang et al. 2009).

The contribution of soil respired carbon to the iWUE–height relationship (Fig. 6) could influence $\delta^{13}C$ assimilation (Figure S1); this is the result of CO_2 originating from soil respiration being depleted in $\delta^{13}C$. In this case, organic matter produced by the lower forest should have lower $\delta^{13}C$ due to an additive effect (Medina and Minchin 1980; Sternberg et al. 1989). However, our study corrected the iWUE values to consider this using the expected $\delta^{13}C_a$ based on CO_2 concentrations measured by a flux tower (Figure S2) (Pataki et al. 2003; Ometto et al. 2002). Leaf $\delta^{13}C$ was positively correlated with $\delta^{13}C_a$ (Figure S1), but the variation in leaf $\delta^{13}C$ along the vertical forest gradient was 7.5, which was greater than the variation in $\delta^{13}C_a$ along the vertical forest profile (Figure S1). The iWUE estimates can be corrected by accounting for the vertical $\delta^{13}C_a$ gradient, as seen in the contrasting iWUE pattern observed in (1) sapling and mature iWUE of understory trees (i.e., *R. publiflora* and *A. longifolia*); (2) sapling and mature individuals growing in the same depleted $\delta^{13}C_a$ atmosphere (Figure S2-d); (3) considering the overstory *C. scleroxylon*, which tends to present a higher iWUE in the sapling stage (Fig. 7); and (4) considering the higher variability found in small understory species. Soil respiration explains no more than 20% of the iWUE trend, and changes in iWUE are primarily related to plant physiological differentiation in response to environmental changes, such as hydraulic strategies and crown illumination (Brienen et al. 2017).

Conclusion

Hydrological acclimation during tree ontogeny is an important mechanism that allows species to change their drought tolerance strategies and the associated iWUE to survive in a seasonal tropical forest. The ontogenetic shift in iWUE is linked to variations in the vulnerability to xylem embolism. We propose that an ontogenetic change in embolism resistance is coupled with the maximization of iWUE in the mature stages of overstory trees. Thus, these functional physiological trait shifts can account for species-specific differences in isotopic discrimination over the growth stages and height strata occupied by a tree throughout its lifetime. This is highly relevant for interpreting changes in iWUE over time related to climate and other factors utilizing isotopic trends in tree rings in dendrochronological studies (Brienen et al. 2017; Vadeboncoeur et al. 2020). This functional ecological capacity for ontogenetic shifts can be understood as an overstory tropical tree species displaying higher drought tolerance during the early ontogenetic phase, similar to understory tree species (regeneration niche—drought-tolerant, low water-use efficiency), and drought avoidance in the mature stage (persistence niche, drought avoidance, and high water-use efficiency).

The significance of our research rests on a pivotal discovery: the potential for tree species in a tropical forest to display responses to climate change that are structured by species' capacities for ontogenetic shifts in water use strategies. These shifts may occur naturally in response to changing growing conditions in height structured canopies but could now offer acclimation capacity in response to shifting average climate conditions in the understory. This important insight, which may be lacking in current vegetation dynamics models (DVMs) (Franklin et al. 2020), raises the question of whether new representations and characterizations of tree ontogenetic stages are imperative. For instance, an investigation into changes in the coefficient of trait variation across environmental gradients and the ontogenetic shifts associated with these changes could enhance the performance of vegetation dynamics models (Westerband et al. 2021). In this regard, it calls for future studies to consider whether tree species that are disproportionately distributed across precipitation gradients in the Amazon Forest (Esquivel-Muelbert et al. in 2016, 2020, Barros et al., 2019; Tavares et al. in 2023), may possess heightened ontogenetic hydrological acclimation capabilities compared to species primarily found in wetter regions within the basin. Integrating this ecological capacity with hydrological niche acclimation along the tree ontogeny in diverse tropical forests into model development and parameterization can improve the prediction of species distribution and ecosystem vegetation responses to drought and climate change (Saleska et al. 2003; Mencuccini et al. 2019; Oliveira et al. 2021; Draper et al. 2021). Ultimately, our results show that synergistic plant physiology, environment, and community dynamics play a role in determining these responses. Finally, the coexistence of these functional strategies may also contribute to the overall and hydrological resilience of tropical seasonal forests owing to hydrological niche complementarity (Silvertown et al. 2015).

Data availability statement

The data that support the findings of this study will be available upon request.

Supplementary Information The online version contains supplementary material available at https://doi.org/10.1007/s11258-023-01361-x.

Acknowledgements We are grateful to the LBA-INPA office in Santarém for management of the LBA flux tower site K67 in the Tapajos National Forest, specially Louro Lima, to Sky Dominguez for logistical support; and to the parataxonomists Ednaldo Augusto Pinheiro Nascimento and Miguel Pastana do Nascimento. We also thank Dr. Marcos Longo for providing the height-diameter model. We thanks to Laboratory at LBA-ECO flux tower, Laboratory of the "Biofísica da Região Amazônica e Modelagem Ambiental"—BRAMA, and in the "Laboratório de Tecnologia da Madeira"—LTM, both in University of Western Pará (UFOPA—"Universidade Federal do Oeste do Pará), for let us use their logistics to process our samples.

Author Contributions MB and formulated the main idea. LFA, RCOJ, and SRXJ helped with floristic, vegetation data, and species identification. MB, VHM, KC, DP, GST, and NP helped with data collection and laboratory analysis. NRC, SRS, and PBC helped with the stable isotope interpretation. PBC processed the stable isotope samples. RCOJ, VHM, JMSM, and RS helped with logistics and laboratory support in Santarém. SRS participated in research coordination and funds management. All authors contributed substantially to writing the manuscript.

Funding This study was financed by the U.S. National Science Foundation (NSF) award DEB-1754803 and DEB-1949894. S.C.S. was supported by NSF award DEB-1754357, synergistic DEB-1950080, and the USDA NIFA. Luciana F. Alves was supported by NSF award DEB 1753973, Deliane Penha was supported by Serrapilheira Institute award 1709-18983. RSO and GST acknowledges CNPq for a productivity scholarship.

Declarations

Competing interests The authors declare no competing interests.

Conflict of interest The authors declare that they have no conflict of interest.

References

Anderegg WRL, Klein T, Bartlett M, Sack L, Pellegrini AFA, Choat B (2016) Meta-analysis reveals that hydraulic traits explain cross-species patterns of drought-induced tree mortality across the globe. PNAS 113:2–7

Barros FV, Bittencourt PRL, Brum M, Restrepo-Coupe N, Pereira L, Teodoro GS, Saleska SR, Borma LS, Christoffersen BO, Penha D, Alves LF, Lima AJN, Carneiro VMC, Gentine P, Lee J, Aragão LEOC, Ivanov V, Leal LSM, Araujo AC, Oliveira RS (2019) Hydraulic traits explain differential responses of Amazonian forests to the 2015 El Nino-induced drought. New Phytol 223:1253–1266

Bittencourt PRL, Oliveira RS, da Costa ACL, Giles AL, Coughlin I, Costa PB, Bartholomew DC, Ferreira LV, Vasconcelos SS, Barros FV, Junior JAS, Oliveira AAR, Mencuccini M, Meir P, Rowland L (2020) Amazonia trees have limited capacity to acclimate plant hydraulic properties in response to long-term drought. Glob Change Biol 26:3569–3584

Bittencourt PR, Pereira L, Oliveira RS (2018) Pneumatic method to measure plant xylem embolism. Bio-Protoc 8(20):e3059–e3059

Brienen RJW, Gloor E, Clerici S, Newton R, Arppe L, Boom A, Bottrell S, Callaghan M, Heaton T, Helama S, Helle G, Leng MJ, Mielikäinen K, Oinonen M, Timonen M (2017) Tree height strongly affects estimates of water-use efficiency responses to climate and CO_2 using isotopes. Nat Commun 8:1–10. https://doi.org/10.1038/s41467-017-00225-z

Brodribb TJ, Holbrook NM, Gutierrez MV (2002) Hydraulic and photosynthetic co-ordination in seasonally dry tropical forest trees. Plant Cell Environ 25(11):1435–1444

Brum M, Vadeboncoeur MA, Ivanov V, Asbjornsen H, Saleska S, Alves LF, Penha D, Dias JD, Aragão LE, Barros F, Bittencourt P, Pereira L, Oliveira RS (2019) Hydrological niche segregation defines forest structure and drought tolerance strategies in a seasonal Amazon forest. J Ecol 107(1):318–333

Cernusak LA, Marshall JD, Comstock JP, Balster NJ (2001) Carbon isotope discrimination in photosynthetic bark. Oecologia 128:24–35

Choat B, Jansen S, Brodribb TJ, Cochard H, Delzon S, Bhaskar R, Bucci SJ, Feild TS, Gleason SM, Hacke UG, Jacobsen AL, Lens F, Maherali H, Martínez-Vilalta J, Mayr S, Mencuccini M, Mitchell PJ, Nardini A, Pittermann J, Pratt RB, Sperry JS, Westoby M, Wright IJ, Zanne AE (2012) Global convergence in the vulnerability of forests to drought. Nature 491:752–755

Cosme LHM, Schietti J, Costa FRC, Oliveira RS (2017) The importance of hydraulic architecture to the distribution patterns of trees in a central Amazonian forest. New Phytol 215:113–125

Costa FR, Schietti J, Stark SC, Smith MN (2023) The other side of tropical forest drought: do shallow water table regions of Amazonia act as large-scale hydrological refugia from drought? New Phytol 237(3):714–733

Dayrell RLC, Arruda AJ, Pierce S, Negreiros D, Meyer PB, Lambers H, Silveira FAO (2018) Ontogenetic shifts in plant ecological strategies. Funct Ecol 32:2730–2741

Ding Y, Nie Y, Chen H, Wang K, Querejeta JI (2021) Water uptake depth is coordinated with leaf water potential, water-use efficiency and drought vulnerability in karst vegetation. New Phytol 229:1339–1353

Domingues TF, Berry JA, Martinelli LA, Ometto JPHB, Ehleringer JR (2005) Parameterization of canopy structure and leaf-level gas exchange for an Eastern Amazonian tropical rain forest (Tapajós national forest, Pará, Brazil). Earth Interact 9:1–23

Draper FC, Costa FRC, Arellano G et al (2021) Amazon tree dominance across forest strata. Nat Ecol Evol. https://doi.org/10.1038/s41559-021-01418-y

Engelbrecht BM, Comita LS, Condit R, Kursar TA, Tyree MT, Turner BL, Hubbell SP (2007) Drought sensitivity shapes species distribution patterns in tropical forests. Nature 447(7140):80–82

Esquivel-Muelbert A, Baker TR, Dexter KG et al (2016) Seasonal drought limits tree species across the Neotropics. Ecography 40:618–629

Esquivel-Muelbert A, Phillips OL, Brienen RJW et al (2020) Tree mode of death and mortality risk factors across Amazon forests. Nat Commun 11:5515

Farquhar GD, O'Leary MH, Berry JA (1982) On the relationship between carbon isotope discrimination and the intercellular carbon dioxide concentration in leaves. Aust J Plant Physiol 9:121–137

Farquhar GD, Lloyd J (1993). Carbon and oxygen isotope effects in the exchange of carbon dioxide between terrestrial plants and the atmosphere. In: Stable isotopes and plant carbon-water relations. Academic Press, pp 47–70

Fernández-de-Uña L, Martínez-Vilalta J, Poyatos R, Mencuccini M, McDowell NG (2023) The role of height-driven constraints

and compensations on tree vulnerability to drought. New Phytol 239(6):2083–2098
Fontes CG, Fine PVA, Wittmann F, Bittencourt PRL, Piedade MTF, Higuchi N, Chambers JQ, Dawson TE (2020) Convergent evolution of tree hydraulic traits in Amazonian habitats: implications for community assemblage and vulnerability to drought. New Phytol 228:106–120
Fonti P, Von Arx G, García-González I, Eilmann B, Sass-Klaassen U, Gärtner H, Eckstein D (2010) Studying global change through investigation of the plastic responses of xylem anatomy in tree rings. New Phytol 185:42–53
Fox J, Weisberg S (2011) An R companion to applied regression, second edition. Sage, Thousand Oaks. http://socserv.socsci.mcmaster.ca/jfox/Books/Companion
Franklin O, Harrison SP, Dewar R, Farrior CE, Brännström Å, Dieckmann U, Pietsch S, Falster D, Cramer W, Loreau M et al. (2020) Organizing principles for vegetation dynamics. Nat plant 6(5):444–453
Garcia MN, Ferreira MJ, Ivanov V, Dos Santos VA, Ceron JV, Guedes AV, Saleska SR, Oliveira RS (2021) Importance of hydraulic strategy trade-offs in structuring response of canopy trees to extreme drought in central Amazon. Oecologia 197:13–24
Giardina F, Konings AG, Kennedy D, Alemohammad SH, Oliveira RS, Uriarte M, Gentine P (2018) Tall Amazonian forests are less sensitive to precipitation variability. Nat Geosci 11(6):405–409
Henn JJ, Damschen EI (2021) Plant age affects intraspecific variation in functional traits. Plant Ecol. https://doi.org/10.1007/s11258-021-01136-2
Ivanov VY, Hutyra LR, Wofsy SC, Munger JW, Saleska SR, De Oliveira RC, De Camargo PB (2012) Root niche separation can explain avoidance of seasonal drought stress and vulnerability of overstory trees to extended drought in a mature Amazonian forest. Water Resour Res 48:1–21
Kotowska MM, Link RM, Röll A, Hertel D, Hölscher D, Waite P-A, Moser G, Tjoa A, Leuschner C, Schuldt B (2021) Effects of wood hydraulic properties on water use and productivity of tropical rainforest trees. Front for Glob Change 3:1–14
Lasky JR, Bachelot B, Muscarella R, Schwartz N, Forero-Montaña J, Nytch CJ, Swenson NG, Thompson J, Zimmerman JK, Uriarte M (2015) Ontogenetic shifts in trait-mediated mechanisms of plant community assembly. Ecology 96:2157–2169
Lenth R (2019) emmeans: estimated marginal means, aka least-squares means. R package version 1.4.1. https://CRAN.R-project.org/package=emmeans
Liu H, Gleason SM, Hao G, Hua L, He P, Goldstein G, Ye Q (2019) Hydraulic traits are coordinated with maximum plant height at the global scale. Sci Adv 5:eaav1332
Longo M (2013). Amazon forest response to changes in rainfall regime: results from an individual-based dynamic vegetation model. Dissertation Thesis, Harvard University
Longo M, Keller M, dos-Santos MN, Leitold V, Pinagé ER, Baccini A, Saatchi S, Nogueira EM, Batistella M, Morton DC (2016) Aboveground biomass variability across intact and degraded forests in the Brazilian Amazon. Glob Biogeochem Cycles 30:1639–1660https://doi.org/10.1002/2016GB005465
Medina E, Minchin P (1980) Stratification of δ13C values of leaves in Amazonian rain forests. Oecologia 45:377–378
Markewitz D, Devine S, Davidson EA, Brando P, Nepstad DC (2010) Soil moisture depletion under simulated drought in the Amazon: impacts on deep root uptake. New Phytol 187:592–607
Mathias JM, Thomas RB (2021) Global tree intrinsic water use efficiency is enhanced by increased atmospheric CO_2 and modulated by climate and plant functional types. Proc Natl Acad Sci 118(7):e2014286118
Nepstad DC, Tohver IM, Ray D, Moutinho P, Cardinot G (2007) Mortality of large trees and lianas following experimental drought in an Amazon forest. Ecology 88(9):2259–2269
McCarroll D, Loader NJ (2004) Stable isotopes in tree rings. Quat Sci Rev 23:771–801
McDowell NG, Allen CD (2015) Darcy's law predicts widespread forest mortality under climate warming. Nat Clim Chang 5:669–672. https://doi.org/10.1038/nclimate2641
McDowell NG, Bond BJ, Dickman LT, Ryan MG, Whitehead D, Meinzer FC, Niinemets Ü (2011) Relationships between tree height and carbon isotope discrimination size- and age-related changes in tree structure and functionhttps://doi.org/10.1007/978-94-007-1242-3_10
McDowell N, Allen CD, Anderson-Teixeira K, Brando P, Brienen R, Chambers J, Christoffersen B, Davies S, Doughty C, Duque A, Espirito-Santo F (2018) Drivers and mechanisms of tree mortality in moist tropical forests. New Phytol 219(3):851–869
Meinzer FC, Johnson DM, Lachenbruch B, McCulloh KA, Woodruff DR (2009) Xylem hydraulic safety margins in woody plants: coordination of stomatal control of xylem tension with hydraulic capacitance. Funct Ecol 23:922–930
Meinzer FC, McCulloh KA (2013) Xylem recovery from drought-induced embolism: where is the hydraulic point of no return? Tree Physiol 33(4):331–334
Mencuccini M (2003) The ecological significance of long-distance water transport: Short-term regulation, long-term acclimation and the hydraulic costs of stature across plant life forms. Plant Cell Environ 26:163–182
Mencuccini M, Manzoni S, Christoffersen B (2019) Modelling water fluxes in plants: from tissues to biosphere. New Phytol 222:1207–1222
Nardini A, Casolo V, Dal Borgo A, Savi T, Stenni B, Bertoncin P, Zini L, Mcdowell NG (2016) Rooting depth, water relations and non-structural carbohydrate dynamics in three woody angiosperms differentially affected by an extreme summer drought. Plant Cell Environ 39:618–627
Oliveira RS, Costa FR, van Baalen E, de Jonge A, Bittencourt PR, Almanza Y, Barros FD, Cordoba EC, Fagundes MV, Garcia S, Guimaraes ZT (2019) Embolism resistance drives the distribution of Amazonian rainforest tree species along hydro-topographic gradients. New Phytol 221(3):1457–1465
Oliveira RS, Eller CB, Barros FDV, Hirota M, Brum M, Bittencourt P (2021) Linking plant hydraulics and the fast-slow continuum to understand resilience to drought in tropical ecosystems. New Phytol. https://doi.org/10.1111/nph.17266
Oliveira-Junior RC, Correa JRV (2001) Caracterização dos solos do município de Belterra, Estado do Pará. Embrapa Amaz Orient Doc 88:39
Olson ME, Soriano D, Rosell JA, Anfodillo T, Donoghue MJ, Edwards EJ, León-Gómez C, Dawson T, Camarero Martínez JJ, Castorena M, Echeverría A, Espinosa CI, Fajardo A, Gazol A, Isnard S, Lima RS, Marcati CR, Méndez-Alonzo R (2018) Plant height and hydraulic vulnerability to drought and cold. Proc Natl Acad Sci 115:7551–7556
Ometto JPHB, Flanagan LB, Martinelli LA, Moreira MZ, Higuchi N, Ehleringer JR (2002) Carbon isotope discrimination in forest and pasture ecosystems of the Amazon Basin, Brazil. Glob Biogeochem Cycles 16:56-1–56-10
Pammenter NW, Vander Willigen C (1998) A mathematical and statistical analysis of the curves illustrating the vulnerability of xylem to cavitation. Tree Physiol 18(8–9):589–593. https://doi.org/10.1093/treephys/18.8-9.589
Pataki DE, Ehleringer JR, Flanagan LB, Yakir D, Bowling DR, Still CJ, Buchmann N, Kaplan JO, Berry JA (2003) The application

and interpretation of Keeling plots in terrestrial carbon cycle research 17(1)
Pereira L, Bittencourt PRL, Pacheco VS, Miranda MT, Zhang Y, Oliveira RS, Groenendijk P, Machado EC, Tyree MT, Jansen S, Rowland L, Ribeiro RV (2020) The pneumatron: an automated pneumatic apparatus for estimating xylem vulnerability to embolism at high temporal resolution. Plant Cell Environ 43:131–142
Pereira L, Oliveira RS, Pereira L, Bittencourt PRL, Oliveira RS, Junior MBM, Barros F V (2016) Plant pneumatics : stem air flow is related to embolism—new perspectives on methods in plant hydraulics Methods Plant pneumatics : stem air flow is related to embolism—new perspectives on methods in plant hydraulics. New Phytol 357–370
Pinheiro J, Bates D, DebRoy S, Sarkar D, R Core Team (2021) _nlme: linear and nonlinear mixed effects models_. R package version 3.1-152. https://CRAN.R-project.org/package=nlme
Power SC, Verboom GA, Bond WJ, Cramer MD (2019) Does a trade-off between trait plasticity and resource conservatism contribute to the maintenance of alternative stable states? New Phytol 223:1809–1819
Pyle EH, Santoni GW, Nascimento HEM, Hutyra LR, Vieira S, Curran DJ, Van Haren J, Saleska SR, Chow VY, Camargo PB, Laurance WF, Wofsy SC (2009) Dynamics of carbon, biomass, and structure in two Amazonian forests. J Geophys Res Biogeosci 114:1–20
R Core Team (2017) R: a language and environment for statistical computing. Vienna, Austria: R Foundation for Statistical Computing. https://www.R-project.org/
Reich PB (2000) Do tall trees scale physiological heights? Trends Ecol Evol 15:41–42
Restrepo-Coupe N, Levine NM, Christoffersen BO, Albert LP, Wu J, Costa MH, Galbraith D, Imbuzeiro H, Martins G, da Araujo AC, Malhi YS, Zeng X, Moorcroft P, Saleska SR (2016) Do dynamic global vegetation models capture the seasonality of carbon fluxes in the Amazon basin? A data-model intercomparison. Glob Chang Biol 1–18
Restrepo-Coupe N, da Rocha HR, Hutyra LR, da Araujo AC, Borma LS, Christoffersen B, Cabral OMR, de Camargo PB, Cardoso FL, da Costa ACL, Fitzjarrald DR, Goulden ML, Kruijt B, Maia JMF, Malhi YS, Manzi AO, Miller SD, Nobre AD, von Randow C, Sá LDA, Sakai RK, Tota J, Wofsy SC, Zanchi FB, Saleska SR (2013) What drives the seasonality of photosynthesis across the Amazon basin? A cross-site analysis of eddy flux tower measurements from the Brasil flux network. Agric for Meteorol 182–183:128–144. https://doi.org/10.1016/j.agrformet.2013.04.031
Rice AH, Pyle EH, Saleska SR, Hutyra L, Palace M, Keller M, De Camargo PB, Portilho K, Marques DF, Wofsy SC (2004) Carbon balance and vegetation dynamics in an old-growth Amazonian forest. Ecol Appl 14
Rijkers T, Pons TL, Bongers F (2000) The effect of tree height and light availability on photosyntheltic leaf traits of four neotropical species differing in shade tolerance. Funct Ecol 14:77–86
Rowland L, da Costa ACL, Galbraith DR, Oliveira RS, Binks OJ, Oliveira AAR, Pullen AM, Doughty CE, Metcalfe DB, Vasconcelos SS, Ferreira LV, Malhi Y, Grace J, Mencuccini M, Meir P (2015) Death from drought in tropical forests is triggered by hydraulics not carbon starvation. Nature 528(7580):119–122
Santos VAHFD, Ferreira MJ, Rodrigues JVFC, Rodrigues JVFC, Garcia MN, Ceron JVB, Nelson BW, Saleska SR (2018). Causes of reduced leaf-level photosynthesis during strong El Niño drought in a Central Amazon forest. Glob Change Biol 4266–4279
Saleska SR, Miller SD, Matross DM (2003) Carbon in Amazon forests: unexpected seasonal fluxes and disturbance-induced losses. Science 302:1554–1557
Signori-Müller C, Oliveira RS, Barros FD, Tavares JV, Gilpin M, Diniz FC, Zevallos MJ, Yupayccana CA, Acosta M, Bacca J, Chino RS (2021) Non-structural carbohydrates mediate seasonal water stress across Amazon forests. Nat Commun 12(1):2310
Silvertown J, Araya Y, Gowing D (2015) Hydrological niches in terrestrial plant communities: a review. J Ecol 103:93–108
Smith MN, Stark SC, Taylor TC, Ferreira ML, de Oliveira E, Restrepo-Coupe N, Chen S, Woodcock T, dos Santos DB, Alves LF, Figueira M, de Camargo PB, de Oliveira RC, Aragão LEOC, Falk DA, McMahon SM, Huxman TE, Saleska SR (2019) Seasonal and drought-related changes in leaf area profiles depend on height and light environment in an Amazon forest. New Phytol 222:1284–1297
Sperry JS, Donnelly JR, Tyree MT (1988) A method for measuring hydraulic conductivity and embolisms in xylem. Plant Cell Environ 11:35–40
Sperry JS, Hacke UG, Oren R, Comstock JP (2002) Water de cits and hydraulic limits to leaf water supply. Environment 251–263
Stark SC, Leitold V, Wu JL, Hunter MO, de Castilho CV, Costa FRC, Mcmahon SM, Parker GG, Shimabukuro MT, Lefsky MA, Keller M, Alves LF, Schietti J, Shimabukuro YE, Brando DO, Woodcock TK, Higuchi N, de Camargo PB, de Oliveira RC, Saleska SR (2012) Amazon forest carbon dynamics predicted by profiles of canopy leaf area and light environment. Ecol Lett 15:1406–1414
Sterck F, Markesteijn L, Schieving F, Poorter L (2011) Functional traits determine trade-offs and niches in a tropical forest community. Proc Natl Acad Sci 108:20627–20632
Sterck FJ, Duursma RA, Pearcy RW, Valladares F, Cieslak M, Weemstra M (2013) Plasticity influencing the light compensation point offsets the specialization for light niches across shrub species in a tropical forest understorey. J Ecol 101:971–980. https://doi.org/10.1111/1365-2745.12076
Sternberg LSL, Mulkey SS, Wright SJ (1989) Ecological interpretation of leaf carbon isotope ratios: influence of respired carbon dioxide. Ecology 70(5):1317–1324
Tang H, Dubayah R (2017) Light-driven growth in Amazon evergreen forests explained by seasonal variations of vertical canopy structure. Proc Natl Acad Sci 114(10):2640–2644
Tavares JV, Oliveira RS, Mencuccini M, Signori-Müller C, Pereira L, Diniz FC, Gilpin M, Marca Zevallos MJ, Salas Yupayccana CA, Acosta M, Pérez Mullisaca FM, Barros FDV, Bittencourt P, Jancoski H, Scalon MC, Marimon BS, Oliveras Menor I, Marimon BH, Fancourt M, Chambers-Ostler A, Esquivel-Muelbert A, Rowland L, Meir P, Lola da Costa AC, Nina A, Sanchez JMB, Tintaya JS, Chino RSC, Baca J, Fernandes L, Cumapa ERM, Santos JAR, Teixeira R, Tello L, Ugarteche MTM, Cuellar GA, Martinez F, Araujo-Murakami A, Almeida E, da Cruz WJA, Del Aguila Pasquel J, Aragão L, Baker TR, de Camargo PB, Brienen R, Castro W, Ribeiro SC, Coelho de Souza F, Cosio EG, Davila Cardozo N, da Costa Silva R, Disney M, Espejo JS, Feldpausch TR, Ferreira L, Giacomin L, Higuchi N, Hirota M, Honorio E, Huaraca Huasco W, Lewis S, Flores Llampazo G, Malhi Y, Monteagudo Mendoza A, Morandi P, Chama Moscoso V, Muscarella R, Penha D, Rocha MC, Rodrigues G, Ruschel AR, Salinas N, Schlickmann M, Silveira M, Talbot J, Vásquez R, Vedovato L, Vieira SA, Phillips OL, Gloor E, Galbraith DR (2023) Basin-wide variation in tree hydraulic safety margins predicts the carbon balance of Amazon forests. Nat 617(7959):111–117. https://doi.org/10.1038/s41586-023-05971-3
Thomas SC, Bazzaz FA (1999) Asymptotic height as a predictor of photosynthetic characteristics in Malaysian rain forest trees. Ecology 80:1607
Tomasella M, Beikircher B, Häberle KH, Hesse B, Kallenbach C, Matyssek R, Mayr S (2018) Acclimation of branch and leaf hydraulics in adult *Fagus sylvatica* and *Picea abies* in a forest through-fall exclusion experiment. Tree Physiol 38:198–211

Vadeboncoeur MA, Jennings KA, Ouimette AP, Asbjornsen H (2020) Correcting tree-ring δ13C time series for tree-size effects in eight temperate tree species. Tree Physiol 40:333–349

Weiner J (2004) Allocation, plasticity and allometry in plants. Perspect Plant Ecol Evol Syst 6:207–215

Westerband AC, Funk JL, Barton KE (2021) Intraspecific trait variation in plants: a renewed focus on its role in ecological processes. Ann bot 127(4):397–410

Wu J, Guan K, Hayek M, Restrepo-Coupe N, Wiedemann KT, Xu X, Wehr R, Christoffersen BO, Miao G, da Silva R, de Araujo AC, Oliveira RC, Camargo PB, Monson RK, Huete AR, Saleska SR (2016) Partitioning controls on Amazon forest photosynthesis between environmental and biotic factors at hourly to inter-annual time scales. Glob Change Biol. https://doi.org/10.1111/gcb.13509

Zhang YJ, Meinzer FC, Hao GY, Scholz FG, Bucci SJ, Takahashi FSC, Villalobos-Vega R, Giraldo JP, Cao KF, Hoffmann WA, Goldstein G (2009) Size-dependent mortality in a Neotropical savanna tree: the role of height-related adjustments in hydraulic architecture and carbon allocation. Plant Cell Environ 32:1456–1466